

Numerical static-load test and earthquake simulation of a cable stayed bridge

Muhammad Ibnu Syamsi^{1*}, Taufiq Ilham Maulana¹, and Chung-Yue Wang²

¹Department of Civil Engineering, Universitas Muhammadiyah Yogyakarta, Jl. Brawijaya, Tamantirto, Kasihan, Bantul, Indonesia

²Department of Civil Engineering, National Central University, No. 300, Zhongda Rd, Zhongli District, Taoyuan City, Taiwan

Abstract. A bridge is an essential component of transportation networks and plays a crucial role in the operation of infrastructure, so maintaining this structure to guarantee the regular operation of bridges in a healthy condition is needed. The establishment of a bridge model numerically is a critical step of the bridge evaluation because many cases of the bridge test can be done numerically. The generated results can then be verified and adjusted with the real or full-scale test. This research aims to establish a numerical model of a cable-stayed bridge and perform numerical bridge tests and earthquake simulations. The targeted bridge is located in Taiwan, and it consists of four spans with three pylons. Static load tests are performed using a truck load set applied at each mid-span. Bridge displacement due to the truckloads is the primary concern of the static load test. Besides, dynamic bridge simulation under earthquake excitation is also simulated. On 18 September 2022, a destructive earthquake of moment magnitude (M_w) 7.1 occurred in Taitung County, southeastern Taiwan. Some infrastructures like bridges and buildings were damaged and even collapsed due to this earthquake. The bridge is simulated using the earthquake history record of the earthquake. The bridge's dynamical system properties are first outputted to see the bridge's natural frequencies and mode shapes. Displacement and stress history responses due to the earthquake excitation at some critical points are also evaluated. The simulation results can be a reference for real bridge testing.

1 Background

Bridges are a crucial element of a nation's ground transportation infrastructure system that transports people and goods from one place to another [1]. Therefore, in order to ensure the regular functioning of bridges in a healthy state, it is important to inspect, maintain, and manage the infrastructural systems. Bridges are designed to operate effectively for their service life duration and sustain the loads specified in the design. A rapid or progressive shift in the in-service load deflection of a structure might indicate structural failure due to factors including fracture, corrosion, support movement, inadequate bearings, inelastic deformation, etc. Bridge deterioration may result from loads, and weather influences [1]. The performance of the structural response in service is determined by deflections, cracking, and inelastic deformations connected to the structure [2]. These performance criteria for serviceability conditions are often to be discussed. AASHTO provides potential limits for live load deflections stated as a fraction of the span length, which is considered to be a span length/800 for regular bridges and a span length/1000 for bridges with pedestrians in urban regions [3]. These restrictions are mostly in place to provide bridge comfort during operating circumstances. Furthermore, measuring deflections provides an important diagnostic tool for assessing the structural health of bridges [2]. In order to

calculate back residual capacity, evaluate in-service performance against expected behavior, or assess the level of damage, the measured deflection response may be included in a bridge finite element model [2].

Regular inspection and load testing are necessary to maintain bridges' structural integrity and safety to give accurate predictions of bridge response and to assist decisions on the most appropriate approach for maintenance and rehabilitation [4-5]. Performing in-situ bridge load tests is essential for determining a structure's well-maintained [6]. The load test was first done to convince the public that a bridge was secure and capable of being used [7]. Load testing is often used to assess existing bridges when traditional analytical approaches can't correctly capture their in-service performance, while some countries still require it for all or specific kinds of newly constructed bridges [8]. Bridge load testing allows for comparing the assumed behaviors in theory with the actual behavior of the bridge under test load [9]. However, AASHTO advises in situ bridge load testing, and it should be emphasized that there are currently no restrictions for bridge load test procedures [10].

Static and dynamic load tests can be split depending on the load applied to the bridge [8]. There are two types of static load tests, proof, and dynamic load tests [11]. Diagnostic testing estimates the structure responses due to certain external loads [12, 13], while proof loads to

*Corresponding author: syamsibnu@umy.ac.id

ensure that the bridge can resist the live loads specified by a standard code without significant stress [14-17].

Recently, a huge earthquake occurred in Taiwan, causing some infrastructure damage and even collapse. A cable-stayed bridge with a total length of 448 m as a crucial element of the transportation network in that area is essential to be evaluated. This research aims to establish the numerical model of the bridge. Static load tests were numerically performed and compared to those obtained from field assessment. Besides, earthquake excitation is simulated to evaluate the bridge's displacement and condition due to the ground motion occurred in Taiwan, September 2022. Some parameters to be considered in this work are static displacements, the bridge's dynamic behaviors, and bridge history responses due to earthquakes. The obtained results can be used as a reference for real bridge testing in the future.

2 Research method

The research method starts by collecting drawing documents and all supporting information related to the bridge construction. Survey to confirm the bridge design is essential for the visual inspection process. Once all that information is collected, a numerical bridge model can be established.

Bridge load tests are conducted to confirm the bridge responses in numerical simulation. The bridge responses are then compared to those obtained through field testing. Some parameters are then adjusted such that the numerical model can reflect the real bridge testing. As the main parameter, bridge deck deflection is the main object to be carried out. Therefore, a bridge load test will be conducted in this work. The test is conducted using a set of loaded trucks. The bridge elevation is measured before and after the truck loading. As a result, relative displacement due to the truckloads can be obtained. The recorded truckload data became the input in the numerical simulation and was applied at the same position as in the real test. Displacement outputted through finite element simulation is then compared to those collected in the field experiment.

Since the measured displacement will be compared to those obtained from the numerical model, thus the detail of the truck weights, including the distance between axles, must be recorded (see an example in Fig. 1). Therefore, the finite element truck input loads could be the same as in the real bridge test.

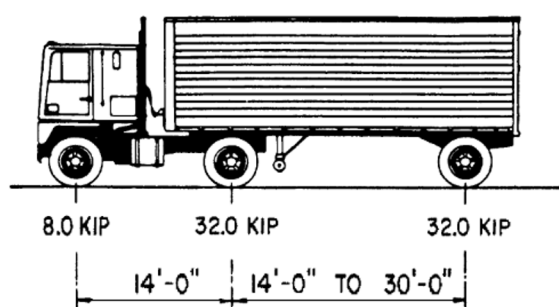


Fig. 1. Design truck by AASHTO [18].

In September 2022, a huge earthquake occurred in Taitung, Taiwan, causing some infrastructure damage. Therefore, bridge evaluation is essential to check whether the bridge is safe or not. For that purpose, earthquake time-history data is essential information. Since the earthquake occurred in all directions, not only along or perpendicular to the bridge axis, the record in the x, y, and z-axis is required.

Earthquake time history record collected in three axes will be the excitation input in the numerical model. Bridge responses subjected to this ground motion are outputted and analyzed. Bending stresses that occurred in main concrete elements, such as the bridge deck and pylon during this earthquake, must be compared with the material strength. Since concrete is weak to tension, thus checking the tension performance during the earthquake is more important than the compression. If the stresses are below the tension limit, the bridge is safe. Otherwise, cracks in the real bridge may happen, requiring a more detailed inspection. Concrete tension is commonly taken as 10 to 15 percent of their compressive strength (ACI 318-14). The time history earthquake acceleration recorded for north-south (NS), east-west (EW), and z (vertical) directions is shown in Fig. 2. Bridge model and all the numerical explorations (truckload tests and earthquake simulation) were done using Midas Civil.

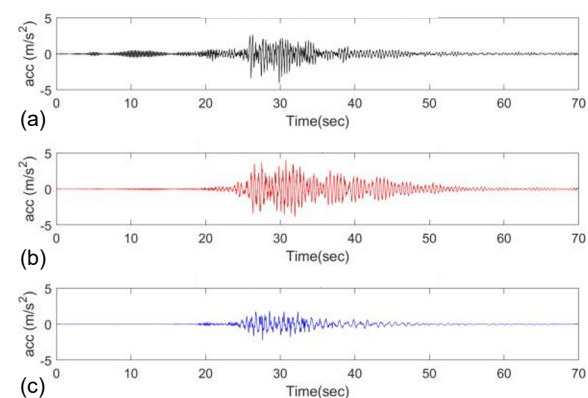


Fig. 2. Earthquake acceleration (a) z-direction (b) NS-direction (c) EW-direction.

3 Bridge information

The bridge discussed in this research is located in Taiwan. The bridge type is cable-stayed, crossing the river, with the total length of the main bridge is 448 m. The bridge consists of four spans and three pylons named P8, P9, and P10. The side spans (spans 1 and 4) have a length of 84 m, and the middle spans (spans 2 and 3) are 140 m. Fig. 3(a) shows the bridge's geometrical condition.

The type of three pylons used in this bridge is a single tower with a single plane-harp system. There are 62 cables connecting the bridge deck to the pylons, where 20 cables on P8 and P10 and 22 cables on P9. Consequently, P9 is higher than P8 and P10.

The concrete tapered box girder is the cross-sectional shape of the bridge deck, as shown in Fig. 3(b),

while the concrete pylon section about the cable is as shown in Fig. 3(c). The pylon cross-section close to the

top surface of the deck is similar to Fig. 3(b) but has a solid section.

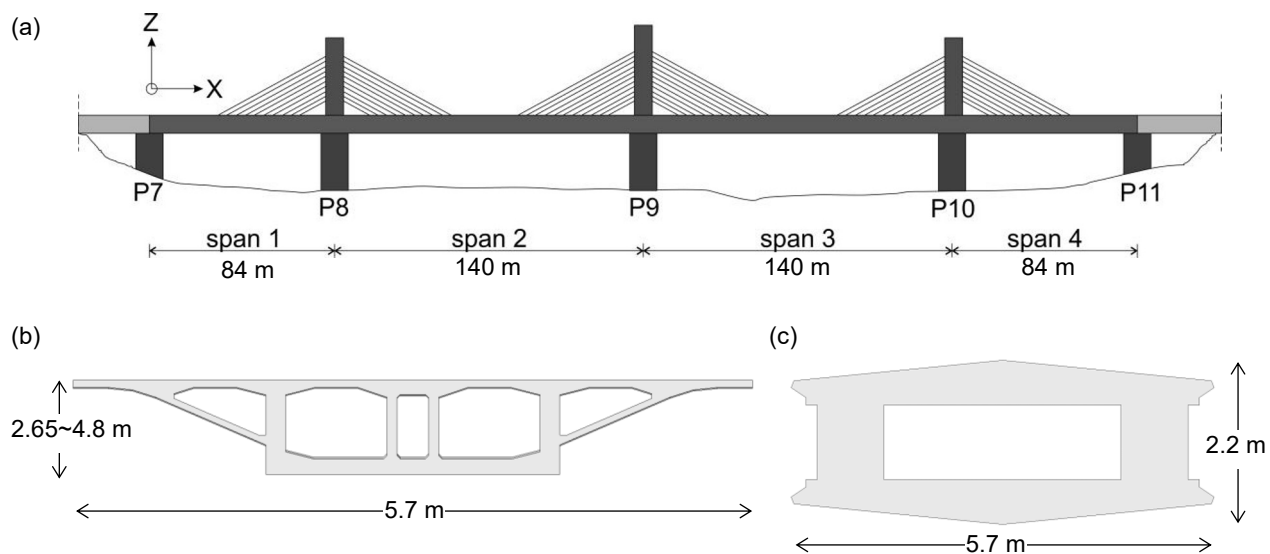


Fig. 3. The bridge geometrical situation (a) bridge span (a) girder cross-section (b) typical pylon cross-section.

4 Bridge model

The bridge was modeled using a finite element software (Midas Civil). The girders and pylons were assigned using frame elements to simplify the global behavior of the bridge, such as the displacements, natural frequencies, and the mode shapes. According to the drawing, the pylon's height is 27.9 m for P8 and P10, while for P9 is 29.9 m. The cable inclination is typically about 17°. In order to include the cable's local modes in the modal analysis, this work modeled the stayed cables as a beam element. The shortest cable was divided into 7 elements, while the longest cable was 17 elements. Pretension force was applied to all of the stayed cables. The cable cross-section is typical for all stayed cables which is 43T-15.2mm ϕ .

Since the main bridge deck is continuous from P7 to P11, and the deck is fixed on each intersection with the bridge pier, thus the bridge pylon and the deck were connected using a rigid link. Non-structural elements such as curb and fence were converted as distributed loads along the bridge. Construction stage sequences were also inputted during the modelling to consider how its structural system, boundary conditions, and material qualities have changed through time. Consequently, time-depending materials were also defined in this study. Fig. 4 displays the 3D model of the bridge.

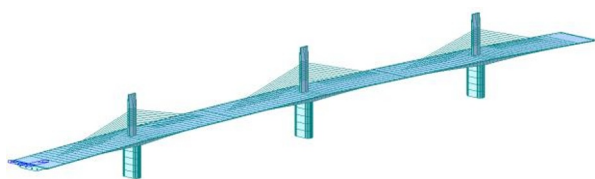


Fig. 4. 3D finite element model.

5 Results and discussion

5.1 Static load test

Bridge load tests were carried out at night when traffic flow was minimal, and the bridge operational condition was stopped to neglect the influence of the other vehicle. The loads consist of four trucks (two each way) facing the same direction, as shown in Fig. 5(a). There were 4 loading positions in this experiment, where each loading position was located on each midspan. Those loads are applied at midspan simultaneously. Once the deflection record is finished, then move to the next span. The weights and the distance between axles measured of all trucks were presented in Tables 1-2, respectively. The W_1 to W_4 and L_1 to L_3 can be observed in Fig. 5(b).

The bridge displacements due to the truckloads were measured using a total station with a total of 40 point measurements. These displacements were obtained by subtracting the bridge elevation before and after the loading trucks were applied. Consequently, the displacements outputted from the field testing were relative displacements due to the loading trucks.

These truck weights and configurations were applied to the bridge model that has been developed. A comparison between the finite element model and bridge deck vertical displacement due to the truckloads is shown in Fig. 6.

In Fig. 6, TS1 to TS4 represent the displacement due to the truckloads on spans 1 to span 4 generated from finite element simulation. The M-TS1 to M-TS4 represents the displacement obtained from field measurement for truckloads applied on spans 1 to 4. The dashed-dot lines indicate the measured displacements at the specific span where the truckloads were applied. Whereas the continuous lines stand for the displacement curves along the bridge spans due to the truckloads

obtained from the finite element. As shown in this figure, the measured displacement curves have a similar trendline to those obtained from the finite element model, where the dashed curves were located about the continuous curves.

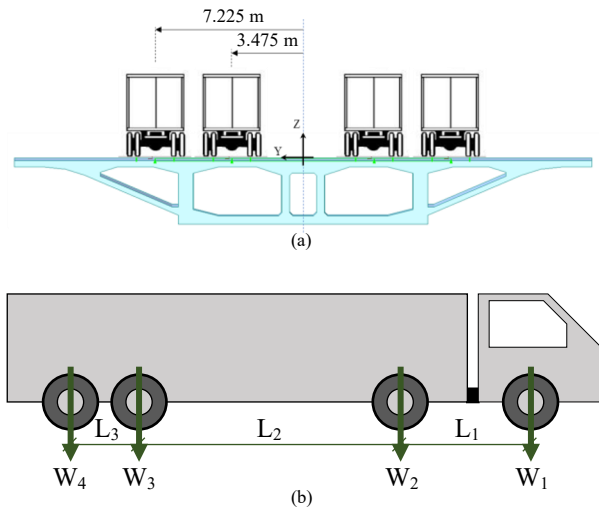


Fig. 5. Truck loads configuration.

In the side spans (spans 1 and 4), the maximum displacement obtained from either measurement or finite element model is about the same value. However, it is shown on the midspan that the bridge deflections obtained using finite element are larger than those from field measurement, where the highest gap between

measurement and finite element is 5.33 mm, where the mean of all deviation is 1.18 mm. Smaller deflection indicates that the deflection is safer. Typically, a bridge reacts to loads more effectively in reality than in theory [9]. Besides, it also observed that the deflections due to the truckloads were positive in some measurement points. This phenomenon was unlikely to occur, so it was possibly caused by an error during measurement.

Table 1. Truck weights.

Truck	weight (kg)			
	W ₁	W ₂	W ₃	W ₄
Truck 1	5712.2	8118.1	10037.4	11262.3
Truck 2	5806.5	8252.1	10203.1	11448.3
Truck 3	5695.9	8095	10008.9	11230.3
Truck 4	5715.4	8122.7	10043.1	11268.7

Table 2. Axle length.

Truck	axle distance (cm)		
	L1	L2	L3
Truck 1	317	478	126
Truck 2	320	490	126
Truck 3	318	479	125
Truck 4	316	443	123

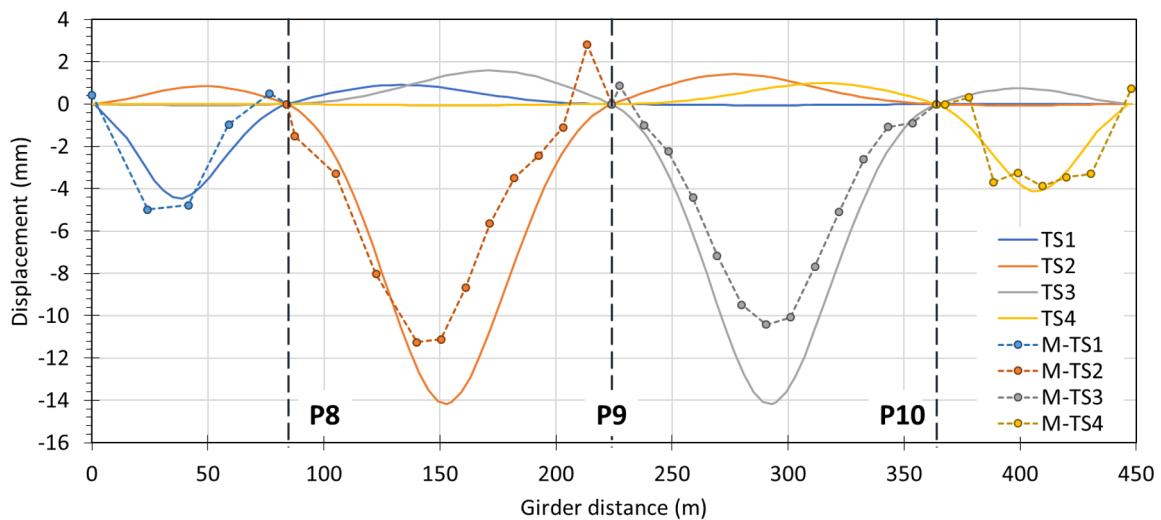


Fig. 6. Displacement comparison between measurement and finite element model.

5.2 Earthquake simulation

The ground acceleration time history recorded during the Taitung earthquake is shown in Fig. 2. The bridge's main axis is not in line with the north-south pole. Thus, some degree angle of the ground motion must be inputted. Displacements on every midspan were outputted in this study. Besides, displacement on the top pylon of P8, P9, and P10 during the ground motion is also observed.

The maximum displacement due to the ground motion about the midspan can be observed in Table 3. The table shows that the maximum displacement occurred on the longest span (Span 2 and Span 3) in the y-direction. Instead of a vertical direction, the bridge span maximum deflection occurred in the horizontal direction. The ground motion in the north-south direction may cause it is more dominant than the other two.

Table 3. Maximum displacement on midspans due to the ground motions.

Span	maximum displacement (cm)		
	DX	DY	DZ
Span 1	0.335	0.555	5.849
Span 2	0.814	7.138	4.006
Span 3	0.884	7.137	3.560
Span 4	0.325	0.555	6.143

Fig. 7 displays the displacement history response on the top of P9 due to the ground motion. As seen in this figure, the displacement history responses of P9 in the x and z-direction are relatively small compared to the y-direction. Aside from the ground motion's amplitude, the large displacement in the y-direction is caused by the weak axis in this direction. Similarly, other pylons have the same behavior, where the maximum displacement occurred in the y-direction. Besides, it is also calculated from Table 4 that the maximum displacement on P9 about the y-axis is 65.5% larger than P8 or P10. P9 has a larger displacement because this pylon is higher than others.

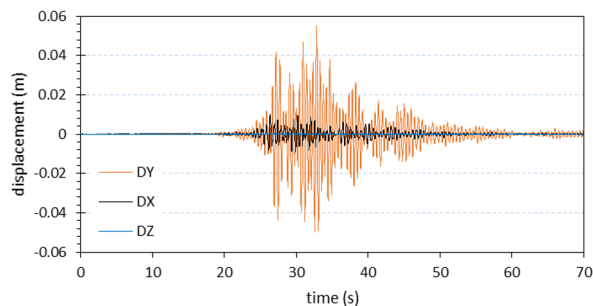


Fig. 7. Displacement history responses on the top of P9.

Table 4. Maximum displacement on top pylons due to the ground motions.

Pier	maximum displacement (cm)		
	DX	DY	DZ
P8	2.487	34.240	0.050
P9	3.564	56.671	0.080
P10	3.386	34.239	0.056

From this comparison, it is obvious that the displacement of P9 is the largest among others. Therefore, it would be better if the bending moment and the stress of P9 were also outputted. More specifically, on the bottom of each pylon, close to the deck surface.

Moment forces history due to the ground motion is shown in Fig. 8 and detailed in Table 5. As can be expected, the highest moment forces are on the P9 since the largest displacement is located on the top of this pylon. Consequently, the biggest stress is also located on P9, as shown in Fig. 9 and Table 6. The maximum bending moment and stress on the deck-level pylon are 210530 km (negative) and 4.155 MPa (positive). Positive and negative indicates the force and stress direction. Positive stress indicates that the pylon suffers tension, while negative for compression. According to

this analysis, it finds that there is a tension force of 4.155 MPa on the base of P9.

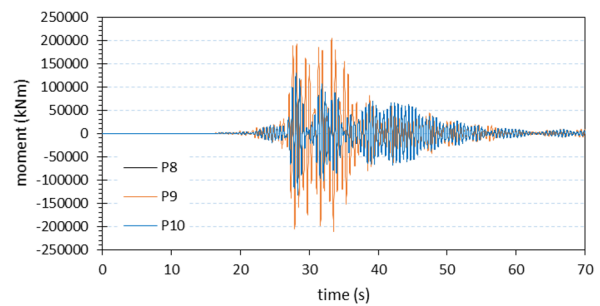


Fig. 8. Moment forces of the deck-level pylon due to the ground motion

Table 5. The maximum bending moment on the deck-level pylon due to the earthquake.

Moment	maximum moment (kNm)		
	P8	P9	P10
Positive	129877.4	204282.1	129903.7
negative	-131837.3	-210530.0	-131840.1

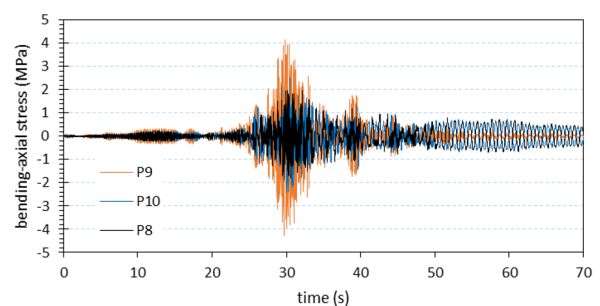


Fig. 9. Bending stress of the deck-level pylon due to the ground motion

Table 6. The maximum bending stress on the deck-level pylon due to the earthquake.

Moment	maximum bending stress (MPa)		
	P8	P9	P10
Positive	1.968	4.155	2.506
negative	-2.507	-1.824	-4.255

According to the ACI 318-14 [19], the allowable tensile stress of concrete can be taken as 10-15% of the compressive strength. If the compressive strength is 35 MPa, the concrete tensile stress is 3.5 to 5.25 MPa. Since the maximum bending stress is 4.155 MPa, the concrete is still safe if the maximum allowable tensile stress of the concrete is taken as 15% (5.25 MPa). But if the maximum is taken as 10% (3.5 MPa), Pylon 9 is not safe, but the other pylon is still under the allowable condition.

6 Conclusion

This study presented establishing a cable-stayed bridge and compared the static load case results with field testing results. The displacement curve is likely similar

between the real test and the finite element model. Besides, the deviation between them is pretty small, with the biggest deviation being 5.33 mm, and the mean is 1.18 mm. The displacement behavior of the finite element model due to the truckloads is quite close to the real test.

Meanwhile, the Taitung earthquake's ground motion in all directions is inputted to study the bridge responses due to this dynamic load. It finds that the top of P9 suffers the highest displacement in the y-direction (56.671 cm) compared to other pylons. Consequently, this large displacement generates bending moment and bending stress. The bending moment and stress at the deck-level pylon obtained from the simulation are 210530 kNm (negative) and 4.155 MPa (positive). If the concrete compressive strength of the pylon is 35 MPa, and the tensile strength is taken as 10%, then the pylon is unsafe. But if it is taken as 15%, then the pylon is still under the concrete allowable condition.

The authors would like to thanks to Universitas Muhammadiyah Yogyakarta for the support of this work.

References

1. H. Cai, O. Abudayyeh, I. Abdel-Qader, U. Attanayake, J. Barbera, E. Almaita, *Advances in Civil Engineering*, 493983 (2012) <https://doi.org/10.1155/2012/493983>
2. K. Helmi, T. Taylor, A. Zarafshan, F. Ansari, *Engineering Structures* **103**, 116-124 (2015) <https://doi.org/10.1016/j.engstruct.2015.09.002>
3. American Association of State Highway and Transportation Officials, LRFD bridge design specifications 2nd edition (AASHTO, 1998)
4. A.S. Ahmad, *Bridge preservation guide: maintaining a state of good repair using cost effective investment strategies* (United States. Federal Highway Administration, 2011) <http://www.fhwa.dot.gov/bridge/preservation/guide/guide.pdf>
5. H.A. Capers, M.M. Valeo, *Transportation research record* **2202**(1), 117-123 (2010) <https://doi.org/10.3141/2202-15>
6. L. Frýba, M. Pirner, *Engineering Structures* **23**(1), 102-109 (2001) [https://doi.org/10.1016/S0141-0296\(00\)00026-2](https://doi.org/10.1016/S0141-0296(00)00026-2)
7. G. Schacht, G. Bolle, S. Marx, *Bautechnik* **93**(2), 85-97 (2016) <https://doi.org/10.1002/bate.201500097>
8. S. Alampalli, D.M. Frangopol, J. Grimson, M.W. Halling, D.E. Kosnik, E.O.L. Lantsoght, D. Yang, Y.E. Zhou, *Journal of Bridge Engineering* **26**(3), 03120002 (2021) [https://doi.org/10.1061/\(ASCE\)BE.1943-5592.0001678](https://doi.org/10.1061/(ASCE)BE.1943-5592.0001678)
9. Transportation Research Board, *Manual for bridge rating through load testing* {NCHRP Project 12-28(13)A, 1998}
10. D.D. Kleinhans, J.J. Myers, A. Nanni, *Journal of Composites for Construction* **11**(5), 545-552 (2007) [https://doi.org/10.1061/\(ASCE\)1090-0268\(2007\)11:5\(545\)](https://doi.org/10.1061/(ASCE)1090-0268(2007)11:5(545))
11. E.O.L. Lantsoght, C. van der Veen, A. de Boer, D. A. Hordijk, *Engineering Structures* **150**, 231-241 (2017) doi: 10.1016/j.engstruct.2017.07.050
12. Y.J. Kim, R. Tanovic, R.G. Wight, *Journal of Performance of Constructed Facilities* **23**(3), 190-200 (2009) [https://doi.org/10.1061/\(ASCE\)CF.1943-5509.0000007](https://doi.org/10.1061/(ASCE)CF.1943-5509.0000007)
13. D.V. Jáuregui, P.J. Barr, *Journal of Performance of Constructed Facilities* **18**(4), 195-204 (2004) [https://doi.org/10.1061/\(ASCE\)0887-3828\(2004\)18:4\(195\)](https://doi.org/10.1061/(ASCE)0887-3828(2004)18:4(195))
14. C.V. Aguilar, D.V. Jáuregui, C.M. Newton, B.D. Weldon, T.M. Cortez, *Transportation Research Record* **2522**(1), 90-99 (2015) <https://doi.org/10.3141/2522-09>
15. E. Lantsoght, C. van der Veen, A. de Boer, D.A. Hordijk, *Structural Concrete* **18**(4), 597-606 (2017) <https://doi.org/10.1002/suco.201600171>
16. R. Anay, T.M. Cortez, D.V. Jáuregui, M.K. ElBatouny, P. Ziehl, *Journal of Performance of Constructed Facilities* **30**(4), 04015062 (2016) [https://doi.org/10.1061/\(ASCE\)CF.1943-5509.0000810](https://doi.org/10.1061/(ASCE)CF.1943-5509.0000810)
17. J.R. Casas, J.D. Gómez, *KSCE J Civ Eng* **17**, 556-567 (2013) <https://doi.org/10.1007/s12205-013-0007-8>
18. American Association of State Highway and Transportation Officials, *AASHTO LRFD bridge design specification* (LRFDUS-6, 2012)
19. ACI Committee 318, *Building code requirements for structural concrete and commentary* (ACI 318-14)